

A fast digital image correlation method for deformation measurement

Bing Pan ^{a,*}, Kai Li ^{b,**}

^a Institute of Solid Mechanics, Beihang University, Beijing 100191, China

^b Department of Mechanical Engineering, Shanghai University, Shanghai 200444, China

ARTICLE INFO

Article history:

Received 14 January 2011

Received in revised form

24 February 2011

Accepted 24 February 2011

Available online 16 March 2011

Keywords:

Digital image correlation

Deformation measurement

Sub-pixel

ABSTRACT

Fast and high-accuracy deformation analysis using digital image correlation (DIC) has been increasingly important and highly demanded in recent years. In literature, the DIC method using the Newton–Raphson (NR) algorithm has been considered as a gold standard for accurate sub-pixel displacement tracking, as it is insensitive to the relative deformation and rotation of the target subset and thus provides highest sub-pixel registration accuracy and widest applicability. A significant drawback of conventional NR-algorithm-based DIC method, however, is its extremely huge computational expense. In this paper, a fast DIC method is proposed deformation measurement by effectively eliminating the repeating redundant calculations involved in the conventional NR-algorithm-based DIC method. Specifically, a reliability-guided displacement scanning strategy is employed to avoid time-consuming integer–pixel displacement searching for each calculation point, and a pre-computed global interpolation coefficient look-up table is utilized to entirely eliminate repetitive interpolation calculation at sub-pixel locations. With these two approaches, the proposed fast DIC method substantially increases the calculation efficiency of the traditional NR-algorithm-based DIC method. The performance of proposed fast DIC method is carefully tested on real experimental images using various calculation parameters. Results reveal that the computational speed of the present fast DIC is about 120–200 times faster than that of the traditional method, without any loss of its measurement accuracy

© 2011 Elsevier Ltd. All rights reserved.

1. Introduction

Development in digital image correlation (DIC) [1,2] in the last thirty years has made it a popular and powerful technique for full-field motion, deformation and shape measurement. As a typical non-interferometric optical metrology with distinct advantages of simple experimental set-up, low-requirement on experimental environment and wide range of applicability, the DIC technique has been widely used for deformation and shape measurement, mechanical parameters characterization as well as numerical–experimental and theoretical–experimental cross validations.

The basic principle of the standard and most widely used subset-based DIC method is rather simple, namely matching (or tracking) the same subsets (or subimages) located in the reference image and deformed image to retrieve the full-field displacements. Although the DIC technique is simple in principle and implementation, two main challenges are always presented in its practical applications. One is the sub-pixel registration

accuracy, and the other is the computational efficiency. Naturally, the ultimate objective of DIC technique is to achieve high-accuracy and real-time deformation and/or shape measurements.

As for the first challenge (i.e., the accuracy and precision of DIC measurements), various factors, such as speckle pattern [3,4], subset size [5], correlation criterion [6], shape function [7–10], sub-pixel interpolation scheme [9–12] as well as sub-pixel registration algorithm [13,14], which have important influences on the registration accuracy of DIC, have been thoroughly investigated by various researchers. Currently, an iterative spatial domain cross-correlation algorithm (e.g., a Newton–Raphson (NR) algorithm), combined with a robust matching criterion (e.g., a zero-mean normalized cross-correlation criterion, ZNCC) and a high-accuracy sub-pixel interpolation algorithm (e.g., a bicubic interpolation scheme), has been considered as a gold standard for accurate sub-pixel motion detection. By taking the relative deformation and rotation of the target subset into consideration, the NR algorithm is capable of providing highest sub-pixel registration accuracy and widest applicability. In the past years, the original NR algorithm [15] has been improved by various researchers [16–21] for reducing its complexity, improving its robustness and extending its applicability. Despite being the most widely used as well as the most accurate algorithm for sub-pixel motion estimation, one significant drawback of NR algorithm, however, remains to be its

* Corresponding author.

** Corresponding author.

E-mail addresses: panb04@mails.tsinghua.edu.cn (B. Pan), likai@shu.edu.cn (K. Li).

¹ These two authors contribute equally to the paper.

extremely huge computational cost. As various time-critical applications of DIC have been increasingly important in recent years, a fast DIC method using the high-accuracy NR algorithm is therefore highly desirable.

This reason why the NR-algorithm-based DIC method is computationally expensive can be attributed to the following two aspects. First, the NR algorithm is a non-linear numerical optimization algorithm, which requires an accurate initial guess to converge accurately and rapidly [16]. Conventionally, the initial guess of each calculation point is separately estimated by performing a simple but time-consuming exhaustive integer displacement searching scheme within the pre-specified search range of the deformed image [15–17]. Various techniques [22–26], such as a frequency domain correlation based on FFT [22], a nested searching scheme [23] and a sum-table approach [24–26], have been proposed to speed the calculation of the integer displacement searching; however, these techniques at least have two shortcomings: (1) they are hard or unable to deal with a specimen subject to large rotation and/or deformation; (2) they more or less consume certain amount of calculation time, despite being relatively computational efficient. Second, during each step of iterative optimization using NR algorithm, certain sub-pixel interpolation algorithm must be used repeatedly to reconstruct the intensity as well as intensity gradients at each sub-pixel location for the displaced pixel points of target subset. The sub-pixel interpolation calculation of a pixel point of certain reference subset is not only performed in each round of iteration, but also needs to be carried out for the same pixel point appeared in adjacent reference subsets, as the interrogated subsets defined in the reference image are normally highly overlapping. The repeated interpolation calculation performed at sub-pixel locations, in particular, consumes most redundant calculations of the existing NR-algorithm-based DIC method.

In this paper, we will demonstrate that the above two calculations are either unnecessary or redundant. A fast DIC method is proposed to achieve fast yet accurate deformation analysis by effectively eliminating the aforementioned redundant calculations involved in the conventional NR-algorithm-based DIC method. The proposed fast DIC method includes the following two simple but effective approaches. First, a reliability-guided displacement scanning strategy is employed to completely avoid the time-consuming integer-displacement searching calculation by ensuring reliable and accurate initial guess transfer between adjacent points. Second, a pre-computed global interpolation coefficient look-up table is employed to eliminate repetitive interpolation calculation at sub-pixel locations. These two approaches effectively eliminate the repeating redundant calculations of existing NR-algorithm-based DIC method and substantially increase its calculation efficiency. To validate its performance, the proposed fast DIC method is carefully

tested on real experimental images using various calculation parameters. The results show that the proposed fast DIC method is able to process more than 5400 points per second using a subset of 21×21 pixels and a grid step of 5 pixels. It is approximately 120–200 times faster than the existing NR-algorithm-based DIC method, depending on the specific calculation parameters used, on the condition of maintaining its measurement accuracy. Therefore, high-accuracy deformation measurement using DIC can be achieved at very low computational cost.

2. Principles of DIC using NR algorithm

2.1. Fundamental principles of DIC method

In practical implementation of DIC, a region of interest (ROI) must be specified in the reference image first and is further divided into evenly spaced virtual grids. The displacements are computed at each point of the virtual grids to obtain full-field deformation. The basic principle of the standard subset-based DIC is schematically illustrated in Fig. 1. To accurately track motion of each point of interest, a square reference subset of $(2M+1) \times (2M+1)$ pixels centered at the interrogated point $P(x_0, y_0)$ from the reference image is chosen and used to track its corresponding location in the target image. The tracking or matching process is achieved by searching the extreme location of a pre-defined similarity criterion, commonly called correlation criterion. Once the location of the target subset with maximum similarity is found in the deformed image, the displacement components of the reference and target subset centers can be determined. The same tracking procedure is repeated on the other points of interest to obtain full-field displacement of the ROI. It is necessary to note that, to get a balance between high-spatial resolution and computational efficiency, the distance between neighboring virtual grids, also known as grid step, is normally selected to be much smaller than the subset size. In other words, the interrogated subsets overlap each other.

To better evaluate the similarity degree of reference and target subsets and obtain accurate displacement estimation for the reference subset center point, the following Zero-mean Normalized Sum of Squared Differences (ZNSSD) criterion [18], which is insensitive to the scale and offset changes in illumination lighting fluctuations, is utilized in this work:

$$C_{\text{ZNSSD}}(\mathbf{p}) = \sum_{i=-M}^M \sum_{j=-M}^M \left[\frac{f(x_i, y_j) - f_m}{\sqrt{\sum_{i=-M}^M \sum_{j=-M}^M [f(x_i, y_j) - f_m]^2}} - \frac{g(x'_i, y'_j) - g_m}{\sqrt{\sum_{i=-M}^M \sum_{j=-M}^M [g(x'_i, y'_j) - g_m]^2}} \right]^2 \quad (1)$$

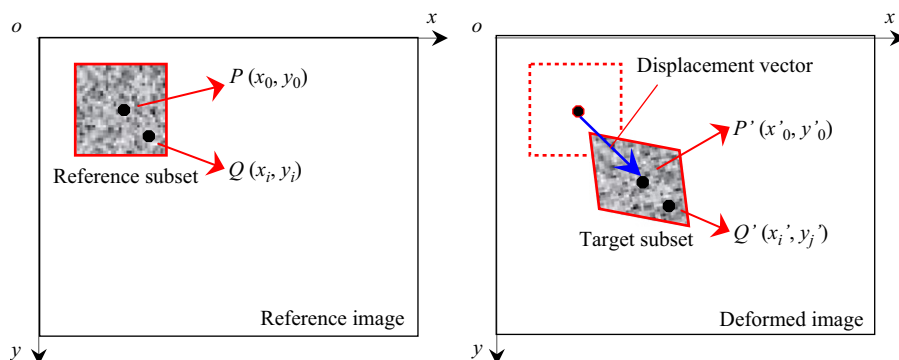


Fig. 1. Basic principle of subset-based DIC method: tracking the same subsets in the reference and deformed image yields displacement vector of the reference subset center.

where \mathbf{p} denotes the desired deformation vector; $f(x_i, y_j)$ is the gray level intensity at coordinates (x_i, y_j) in the reference subset of the reference image and $g(x'_i, y'_j)$ is the gray level intensity at coordinates (x'_i, y'_j) in the target subset of the deformed image;

$$f_m = \frac{1}{(2M+1)^2} \sum_{i=-M}^M \sum_{j=-M}^M [f(x_i, y_j)] \quad \text{and}$$

$$g_m = \frac{1}{(2M+1)^2} \sum_{i=-M}^M \sum_{j=-M}^M [g(x'_i, y'_j)]$$

are the mean intensity values of reference and target subsets, respectively.

It is worth noting that the ZNSSD correlation coefficient is actually related to the commonly used ZNCC coefficient according to the equation of $C_{ZNCC}(\mathbf{p}) = 1 - 0.5 \times C_{ZNSSD}(\mathbf{p})$. The ZNCC coefficient that falls into a range of $[-1, 1]$ is more straightforward to show the similarity degree between the reference subset and target subset. However, the optimization of ZNSSD using NR algorithm is much easier. So, the ZNSSD criterion is optimized using NR algorithm to determine the displacement components of each calculation point. Then, the ZNSSD coefficient is converted to the ZNCC coefficient according to their relations. In the following section, the optimized ZNCC coefficient of calculated points will be used as a reliability (or quality) index to ensure reliable initial guess transfer among consecutive points. As such, the integer displacement scheme can be avoided, leading to significant save in computation time.

In Fig. 1 the point $Q(x_i, y_j)$ in the reference subset can be mapped to the point $Q'(x'_i, y'_j)$ in the target subset according to the so-called “displacement mapping function”. If the subset is sufficiently small, the subset deformation pattern can be well approximated with the commonly used first-order displacement mapping function [15]

$$\begin{aligned} x'_i &= x_0 + \Delta x_i + u + u_x \Delta x_i + u_y \Delta y_j \\ y'_j &= y_0 + \Delta y_j + v + v_x \Delta x_i + v_y \Delta y_j \end{aligned} \quad (2)$$

where u and v are the displacement components for the subset center P in the x and y directions, respectively. The terms Δx_i and Δy_j are the distances from the subset center P to point Q ; and u_x, u_y, v_x and v_y are the displacement gradient components for the subset.

2.2. Optimization of ZNSSD criterion using Newton–Raphson algorithm

It is clear that the ZNSSD criterion is a non-linear function of six unknown parameters. Eq. (1) can be optimized to get the desired in-plane displacement components in the x and y directions using the following classic NR iteration algorithm [18].

$$\mathbf{p} = \mathbf{p}_0 - \frac{\nabla C(\mathbf{p}_0)}{\nabla \nabla C(\mathbf{p}_0)} \quad (3)$$

where \mathbf{p}_0 is the initial guess of the solution, which is conventionally estimated by performing a simple integer displacement searching in a searching region specified in the deformed image; \mathbf{p} is the next iterative approximation solution; $\nabla C(\mathbf{p}_0)$ is the gradients of correlation coefficient and $\nabla \nabla C(\mathbf{p}_0)$ is the second-order derivative of correlation coefficient, also known as Hessian matrix.

To simplify the calculation of Eq. (3), $\nabla C(\mathbf{p}_0)$ and $\nabla \nabla C(\mathbf{p}_0)$ can be further rewritten as follows without any loss of accuracy [16,18]:

$$\nabla C(\mathbf{p}_0) \cong -2 \sum_{i=-M}^M \sum_{j=-M}^M \left\{ \left[\frac{f(x_i, y_j) - f_m}{\Delta f} - \frac{g(x'_i, y'_j) - g_m}{\Delta g} \right] \frac{\nabla g(x'_i, y'_j)}{\Delta g} \right\} \quad (4)$$

$$\nabla \nabla C(\mathbf{p}_0) \cong 2 \sum_{i=-M}^M \sum_{j=-M}^M \left[\frac{1}{(\Delta g)^2} \nabla g(x'_i, y'_j)^T \nabla g(x'_i, y'_j) \right] \quad (5)$$

It is clear that the coordinates of displaced pixels, i.e., (x'_i, y'_j) of Eqs. (4) and (5), in deformed subset, can assume sub-pixel values. It should be noted first that the local area of 2×2 pixels around each considered sub-pixel location is referred to as an interpolation block hereafter. As no gray level information is available between pixels in digital images, therefore in the realization of NR algorithm, an interpolation scheme is needed to reconstruct its intensity and intensity gradients from it adjacent integer pixels. The selection of interpolation scheme is considered as a key factor of NR method, since it directly affects its calculation accuracy and convergence character. In this study, the generalized bicubic interpolation scheme [27,28] is implemented to determine the gray values and first-order gray gradients at sub-pixel locations as follows:

$$\begin{aligned} g(x, y) &= \sum_{m=0}^3 \sum_{n=0}^3 \alpha_{mn} x^m y^n \\ g_x(x, y) &= \sum_{m=1}^3 \sum_{n=0}^3 \alpha_{mn} m x^{m-1} y^n \\ g_y(x, y) &= \sum_{m=0}^3 \sum_{n=1}^3 \alpha_{mn} n x^m y^{n-1} \end{aligned} \quad (6)$$

In bicubic interpolation, the unknown 16 coefficients, i.e., $a_{00}, a_{01}, \dots, a_{33}$, of Eq. (6) can be determined by the gray intensity of the neighboring 4×4 pixels centered at the sub-pixel location. It should be emphasized here that, the 16 coefficients remain the same for each interpolation block, regardless of the specific sub-pixel locations within it.

3. Fast NR algorithm for DIC method by avoiding redundant calculations

3.1. Reliability-guided displacement scanning scheme to avoid integer displacement searching calculation

It is necessary to mention that, as a non-linear optimization algorithm, the NR algorithm requires an accurate initial guess to converge rapidly and accurately. The convergence radius was estimated to be smaller than a few pixels by Vendroux and Knauss [16]. Conventionally, the initial guess of each point of interest is estimated separately by a simple but time-consuming integer displacement searching scheme either performed in spatial domain or in frequency domain based on FFT. Several approaches [22–26] have also been proposed by various researchers to speed the calculation of integer-pixel displacement searching. However, the techniques for integer displacement estimation at least have two shortcomings: (1) they are unable to deal with specimens subjected to large rotation and/or deformation; (2) they are rather computational intensive and therefore time-consuming.

In this work, a reliability-guided displacement tracking scheme is adopted to entirely avoid the computational cost involved in integer displacement searching. With this approach, the correlation calculation begins with a selected seed point (or starting point). As for the seed point, its initial guess is detected through the simple integer-pixel displacement searching process or manually [1,29], subsequently the corresponding sub-pixel displacements can be refined using NR algorithm. Then, the determined displacements as well as the displacement gradients of the point can be directly used as the initial estimate of subset parameters for the next point of investigation according to the continuous deformation assumption [20,21]. This procedure is then repeated to analyze the entire field of displacement or deformation. It is quite important to note here that the calculation path of DIC is guided by the ZNCC coefficient of computed points,

instead of a simple pointwise scanning strategy performed along each column or row. That means the neighbors of the point with highest ZNCC coefficient will be processed first. As the ZNCC coefficient denotes the reliability of the correlation analysis, this novel displacement scanning strategy ensures reliable initial guess transfer between consecutive points, and is referred as to reliability-guided digital image correlation (RG-DIC) in our recent papers [20,21]. The merits of RG-DIC are twofold: (1) the integer-pixel displacement estimation is entirely avoided and thus the computational efficiency is dramatically increased; (2) the RG-DIC is able to deal with specimen with irregular shape and/or subject to discontinuous deformation. More details of RG-DIC method are not the focus of this work and can be found in Refs. [20,21,30]. In summary, the reliability-guided displacement tracking approach does not require searching of integer-pixel displacements for the entire pixel points defined in the ROI of the reference image; instead, the initial estimation of integer-pixel displacements needs to be performed on a starting pixel point (or seed point) only [20,29]. In this way, the repetitive integer displacement tracking computation involved in the NR-algorithm-based DIC method can be effectively avoided.

3.2. Pre-computed interpolation coefficient look-up table for efficient bicubic interpolation

As can be seen from Eqs.(4) and (5), the gray values, i.e., $g(x'_i, y'_j)$, and first-order gray gradients, i.e., $\nabla g(x'_i, y'_j)$, at sub-pixel locations must be provided during the realization of NR algorithm. It is natural to carry out sup-pixel interpolation for each sub-pixel position when necessary, as used in the conventional NR-algorithm-based DIC method. However, this seemingly straightforward approach is extremely time-consuming, and in general takes most of the computational burden of NR algorithm as shown later. For example, if an average iteration of three times is needed by NR algorithm to converge, thus each pixel with the considered subset should be interpolated repeatedly three times. Also, due to the high overlap between adjacent subsets, the pixel point within one reference subset may also appear in its neighboring reference subsets as indicated in Fig. 2, which means repetitive interpolations should be performed on the same pixel point. Given a reference subset of $(2M+1) \times (2M+1)$ pixels and a grid step of ΔL pixels, each pixel within the considered subset will also be used in the adjacent $\lceil \text{floor}((2M+1)/\Delta L) + 1 \rceil^2$ reference subsets, where $\text{floor}(x)$ denotes the largest integer less than x . If the considered pixel point is displaced to a sub-pixel location, this pixel point will be interpolated for approximately $n_{\text{ave}} \times \lceil \text{floor}((2M+1)/\Delta L) + 1 \rceil^2$ times using the direct method (here the average iteration number is assumed as n_{ave}). In other words, the 16 interpolation coefficients required in Eq. (6) are repeatedly calculated $n_{\text{ave}} \times \lceil \text{floor}((2M+1)/\Delta L) + 1 \rceil^2$ times, which implies redundant calculations.

As noted before, while using bicubic interpolation, the 16 coefficients remain the same for each interpolation block, regardless of the specific sub-pixel locations within it. The fact enlightens us to build a global look-up table for each interpolation block of the deformed image prior to NR iteration computation. That means all the unknown 16 interpolation coefficients required in Eq. (6) are pre-computed and saved in a global look-up table before the iteration calculation using NR algorithm. Once one pixel point falls into certain block, these computed interpolation coefficients are directly adopted to reconstruct the intensity and intensity gradients at sub-pixel locations. In this way, the construction of interpolation coefficients should be performed once only, rather than $n_{\text{ave}} \times \lceil \text{floor}((2M+1)/\Delta L) + 1 \rceil^2$ times, for each interpolation block. For instance, if the subset is chosen as 21×21 pixels and the grid step is set as 5 pixels, the interpolation times is

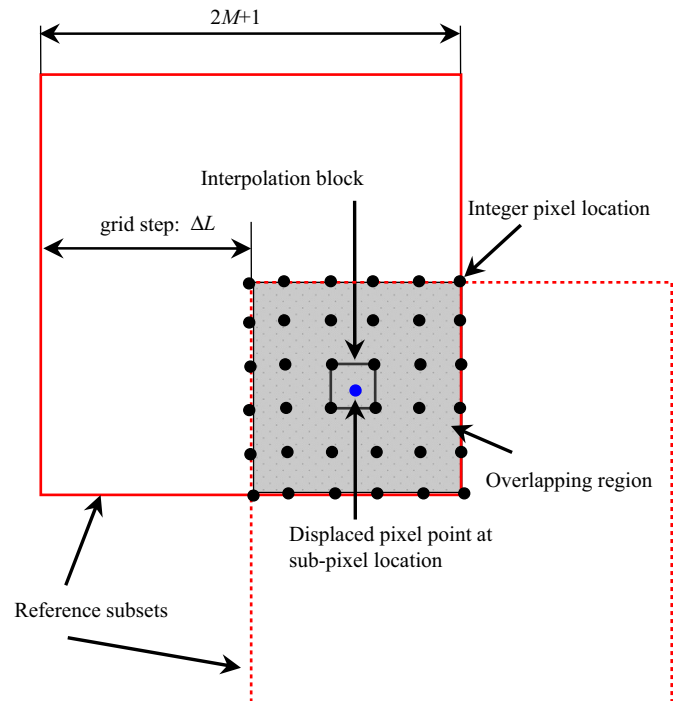


Fig. 2. Schematic diagram showing redundant interpolation in existing direct NR algorithm: The displaced pixel point (blue dot) repeatedly appears at adjacent subsets (dashed line) as the reference subsets defined in reference image overlap each other, which means redundant interpolation calculations during the optimization of various subsets. (For interpretation of the references to color in this figure legend, the reader is referred to the web version of this article.)

reduced from 75 times to merely 1 time. Apparently, a higher overlap between consecutive subsets, which means a larger subset size or a smaller grid step, will further increase the computation efficiency of the proposed method.

4. Experimental verification

The proposed fast DIC method is tested using real experimental images shown in Fig. 3. The two images, with a resolution of 768×576 pixels at 256 gray levels, were recorded from a three-point bending experiment. A rectangular area in the middle of the reference image is chosen to be the region of interest. In following, C++ language was used to realize the proposed fast DIC method, the RG-DIC method and the traditional NR-algorithm-based DIC method, and all the calculations were performed on a personal Pentium Dual E8400 computer with 3.0 GHz main frequency.

To clearly demonstrate the speed improvement caused by the reliability-guided displacement scanning scheme and the pre-computed interpolation coefficient table approach, the fast DIC method was also compared with the reliability-guided DIC (RG-DIC) method and the conventional DIC method. In the direct conventional DIC method, a pointwise integer-pixel displacement searching within a searching range of 50×50 pixels was implemented to provide an initial guess for each point of interest. While in the RG-DIC method, the integer displacement searching is only performed for the seed point. As for the rest of the calculation points, the integer displacement searching is avoided by adopting the reliability-guided initial guess transfer scheme [20]. However, the pre-computed interpolation coefficient look-up table approach is not used in the RG-DIC method.

Fig. 4 gives the computed u - and v -directional displacement of the ROI using fast DIC method with a subset of 21×21 pixels and a

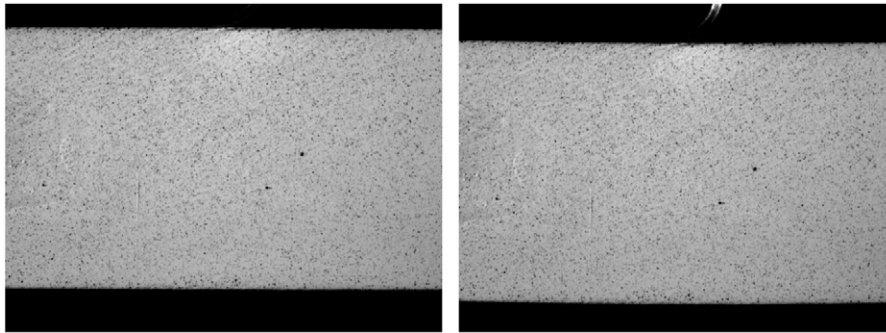


Fig. 3. Reference image (left) and deformed image (right) captured in a three-point bending experiment.

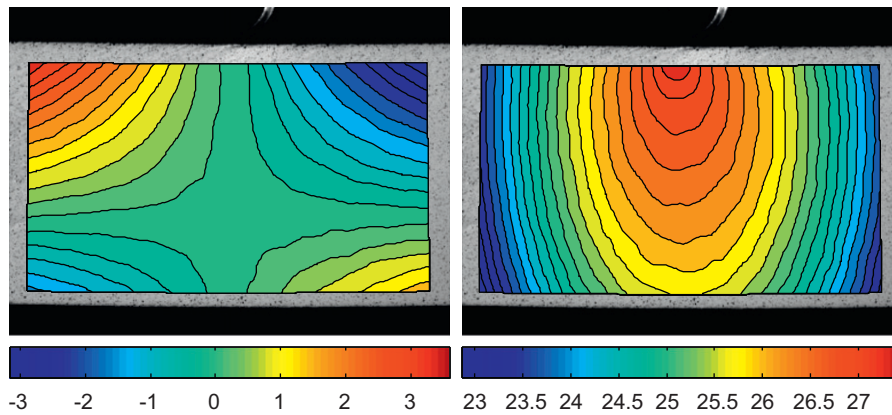


Fig. 4. Computed u -displacement (left) and v -displacement (right) for the three-point bending test.

grid step of 5 pixels. The contours of extracted displacement fields are imposed onto the deformed image to give an intuitive look. In this case, totally 11421 ($=81 \times 121$) points were analyzed and the overall calculation time was equal to 2.11 s, corresponding to a calculation speed of 5489 points/s. Although not shown here, it should be noted that the RG-DIC and the traditional NR-algorithm-based DIC yield identical results, as they are mathematically equivalent, i.e., both computed Eq. (3). The computational speed of the proposed fast DIC method is comparable with that of the commercial DIC software (Vic-2009, Correlated Solutions, Inc., Columbia, USA) [31], while the basic principles of the latter are unclear to us.

Fig. 5 shows the computational speeds of the fast DIC, the RG-DIC and the conventional NR-algorithm-based DIC at different subset sizes. Compared with the traditional DIC method, the fast DIC method and the RG-DIC method increase the computational speed by 175–199 times and 32–38 times, respectively, depending on the subset size used. The results shown in Fig. 5 prove that both the approaches proposed in this work are able to significantly increase the computational speed of direct NR algorithm, but the pre-computed interpolation coefficient table approach is more efficient. Also as can be seen in Fig. 5, the computational speed of all the three algorithms decreases steadily with the increase of the subset size used. For instance, as the subset size increases from 21×21 to 61×61 pixels, the computational speed of fast DIC method decreases from 5489 to 659 points/s. Nevertheless, the fast DIC method is still 175 times fast than that of the conventional method in this case. This can be explained by the fact that a larger subset involves more pixels to be analyzed. Although the interpolation coefficients of each interpolation block are required only once, the time needed for reconstruction of intensity and intensity gradients at sub-pixel locations is linearly proportional to the total number of pixels to be processed.

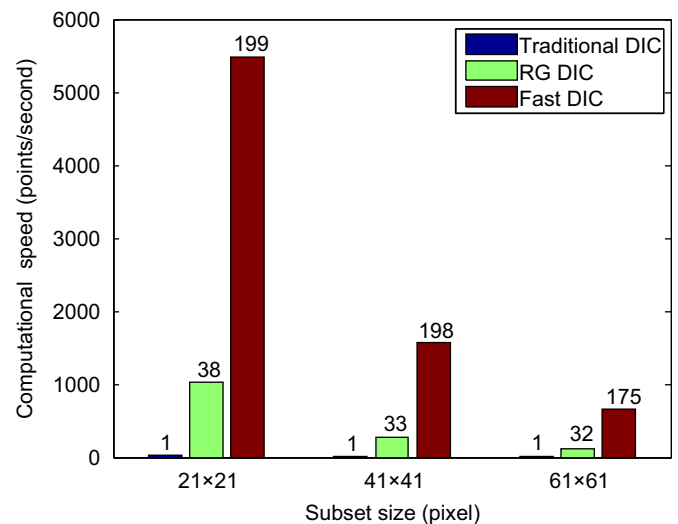


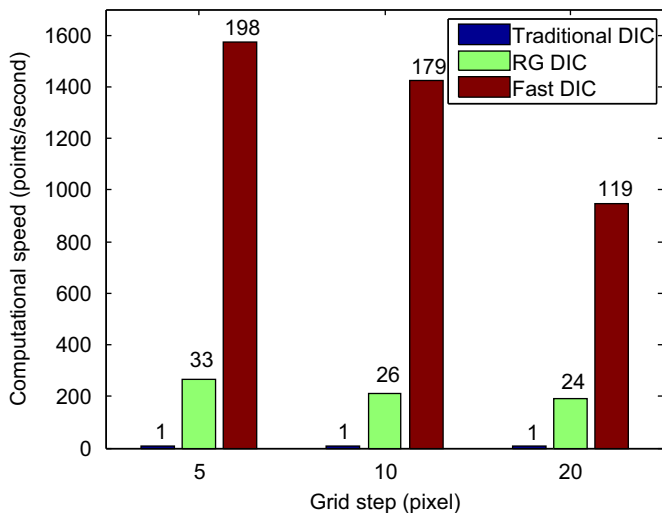
Fig. 5. Comparison of computational speed of the traditional DIC method, RG-DIC method and the fast DIC method using various subset sizes. The numbers on each bar denote the computational speed ratios of RG-DIC method and the fast DIC method to the traditional DIC method.

The average iteration and detailed computational time of the used three NR algorithms are given in Table 1. Compared with the initial guess in terms of integer displacement estimated by implementing a simple searching scheme used in traditional NR-algorithm-based DIC method, the initial guesses provide by the reliability-guided displacement scanning scheme are more accurate, leading to a fast converge speed with less iteration number. As shown in Table 1, the average iteration of fast DIC method is only half of that of the conventional method. The fast

Table 1

Comparison of the average iteration and computational time of fast DIC method, the RG-DIC method and the traditional DIC method using various subset sizes.

Subset size (pixels)	Average iteration			Calculation time (s)		
	Traditional DIC	RG-DIC	Fast DIC	Traditional DIC	RG-DIC	Fast DIC
21 × 21	2.463	1.044	1.044	415.03	11.12	2.11
41 × 41	2.455	1.031	1.031	1436.61	42.97	7.35
61 × 61	2.472	1.025	1.025	3029.48	95.18	17.32

**Fig. 6.** Comparison of computational speed of the traditional DIC method, the RG-DIC method and the fast DIC method using various grid steps. The numbers on each bar denote the computational speed ratios of RG-DIC method and the fast DIC method to the traditional DIC method.

convergence speed clearly indicates the advantages of the reliability-guided displacement scanning scheme.

Fig. 6 compares the computational speeds of the fast DIC method, RG-DIC method and the conventional DIC method at different grid steps, ranging from 5 to 20 pixels, for a fixed subset size of 41×41 pixels. As shown, the computational speed of direct NR algorithm is almost invariant to the grid step used; while the computational speed of the RG-DIC method and in particular the fast DIC method decrease as the grid step size increases. In other words, the efficiency of the fast DIC method decreases when a large grid step used for calculation. This is mainly because of the reduced subset overlaps when the grid step increases. However, when there is no overlap between consecutive reference subsets (i.e., the grid step equals to half subset size), the computational efficiency of the fast DIC method is still substantially higher than that of the conventional method. Specifically, the fast DIC method is approximately 120 times faster than the conventional method, when the grid step is set to be 20 pixels (i.e., half of the subset size).

5. Concluding remarks

A time-efficient fast DIC method based on high-accuracy Newton–Raphson algorithm is proposed in this paper for fast and accurate deformation measurement. By use of a reliability-guided displacement tracking scheme, reliable and accurate initial guess transfer between consecutive points of interest can be achieved. As a result, time-consuming integer displacement required in conventional DIC method is therefore entirely avoided in the proposed fast DIC method. Also, by building a look-up table for the interpolation coefficients of each interpolation block of

2×2 pixels in the deformed image, redundant sub-pixel interpolation calculation can be drastically decreased in the proposed fast DIC method. Experimental results reveal that the proposed fast DIC method is about 120–200 times faster than the conventional NR-algorithm-based DIC method without any loss of its measurement accuracy, thus allowing for high-accuracy deformation measurement at low computational cost.

Acknowledgments

This work is supported by the National Natural Science Foundation of China (NSFC) under grants 11002012 and 10902066, the Science Fund of State Key Laboratory of Automotive Safety and Energy under grant KF10041, the Specialized Research Fund for the Doctoral Program of Higher Education under grant 20101102120015 and the Fundamental Research Funds for the Central Universities.

References

- [1] Pan B, Qian KM, Xie HM, Asundi A. Two-dimensional digital image correlation for in-plane displacement and strain measurement: a review. *Meas Sci Technol* 2009;20:062001.
- [2] Sutton MA, Orteu JJ, Schreier HW. *Image Correlation for Shape, Motion and Deformation Measurements*. Springer; 2009.
- [3] Lecompte D, Smits A, Bossuyt S, Sol H, Vantomme J, Hemelrijck DV, et al. Quality assessment of speckle patterns for digital image correlation. *Opt Lasers Eng* 2006;44(11):1132–45.
- [4] Pan B, Lu ZX, Xie HM. Mean intensity gradient: an effective global parameter for quality assessment of the speckle patterns used in digital image correlation. *Opt Lasers Eng* 2010;48(4):469–77.
- [5] Pan B, Xie HM, Wang ZY, Qian KM, Wang ZY. Study of subset size selection in digital image correlation for speckle patterns. *Opt Express* 2008;16(10):7037–48.
- [6] Pan B, Xie HM, Wang ZY. Equivalence of digital image correlation criteria for pattern matching. *Appl Opt* 2010;49(28):5501–9.
- [7] Lu H, Cary PD. Deformation measurement by digital image correlation: implementation of a second-order displacement gradient. *Exp Mech* 2000;40(4):393–400.
- [8] Schreier HW, Sutton MA. Systematic errors in digital image correlation due to undermatched subset shape functions. *Exp Mech* 2002;42(3):303–10.
- [9] Lava P, Cooreman S, Coppieters S, Strycker MD, Debruyne D. Assessment of measuring errors in DIC using deformation fields generated by plastic FEA. *Opt Laser Eng* 2009;47(7–8):747–53.
- [10] Lava P, Cooreman S, Debruyne D. Study of systematic errors in strain fields obtained via DIC using heterogeneous deformation generated by plastic FEA. *Opt Laser Eng* 2010;48(4):457–68.
- [11] Schreier HW, Braasch JR, Sutton MA. Systematic errors in digital image correlation caused by intensity interpolation. *Opt Eng* 2000;39(11):2915–21.
- [12] Wang YQ, Sutton MA, Bruch HA, Schreier HW. Quantitative error assessment in pattern matching: effects of intensity pattern noise, interpolation, strain and image contrast on motion measurement. *Strain* 2009;45:160–78.
- [13] Pan B, Xie HM, Xu BQ, Dai FL. Performance of sub-pixel registration algorithms in digital image correlation. *Meas Sci Technol* 2006;17(6):15–1621.
- [14] Zhang J, Cai Y, Ye W, Yu TX. On the use of the digital image correlation method for heterogeneous deformation measurement of porous solids. *Opt Lasers Eng* 2011;49(2):200–9.
- [15] Bruck HA, McNeil SR, Sutton MA, Peters WH. Digital image correlation using Newton–Raphson method of partial differential correction. *Exp Mech* 1989;29(3):261–7.
- [16] Vendroux G, Knauss WG. Submicron deformation field measurements: part 2. Improved digital image correlation. *Exp Mech* 1998;38(2):86–92.
- [17] Chen J, Zhang X, Zhan N, Hu X. Deformation measurement across crack using two-step extended digital image correlation method. *Opt Lasers Eng* 2010;48(11):1126–31.

- [18] Pan B, Xie HM, Guo ZQ, Hua T. Full-field strain measurement using a two-dimensional Savitzky–Golay digital differentiator in digital image correlation. *Opt Eng* 2007;46(3):033601.
- [19] Pan B, Asundi A, Xie HM, Gao JX. Digital Image correlation using iterative least squares and pointwise least squares for displacement field and strain field measurements. *Opt Lasers Eng* 2009;47(7–8):865–74.
- [20] Pan B. Reliability-guided digital image correlation for image deformation measurement. *Appl Opt* 2009;48(28):1535–42.
- [21] Pan B, Wang ZY, Lu ZX. Genuine full-field deformation measurement of an object with complex shape using reliability-guided digital image correlation. *Opt Express* 2010;18(2):1011–23.
- [22] Chen DJ, Chiang FP, Tan YS, Don HS. Digital speckle-displacement measurement using a complex spectrum method. *Appl Opt* 1993;32(11):1839–49.
- [23] Zhang ZF, Kang YL, Wang HW, Qin QH, Qiu Y, Li XQ. A novel coarse-fine search scheme for digital image correlation method. *Measurement* 2006;39(8):710–8.
- [24] Tsai DM, Lin CT. Fast normalized cross correlation for defect detection. *Pattern Recognition Lett* 2003;24(15):2625–31.
- [25] Huang JY, Pan XC, Peng XL, Zhu T, Qin L, Xiong CY, et al. High-efficiency cell-substrate displacement acquisition via digital image correlation method using basis functions. *Opt Lasers Eng* 2010;48(11):1058–66.
- [26] Luo J, Konofagou EEA. Fast normalized cross-correlation method for motion estimation. *IEEE Trans Ultrason Ferroelectr Control* 2010;57(7):1347–57.
- [27] Wang ZY, Hoang TM, Nguyen DA, Urcinas AC, Magro JR. High-speed digital-image correlation method: comment. *Opt Lett* 2010;35(17):2891.
- [28] <http://en.wikipedia.org/wiki/Bicubic_interpolation>.
- [29] Press William H. *C++ Numerical Algorithms*. Beijing: Publishing House of Electronics Industry; 2003.
- [30] Pan B, Wu DF, Xia Y. High-temperature field measurement by combing transient aerodynamic heating system and reliability-guided digital image correlation. *Opt Lasers Eng* 2010;48(9):841–8.
- [31] <<http://www.correlatedsolutions.com/index.php/products/vic-2d-2009>>.